Inorganic Chemistry

Article

pubs.acs.org/IC

Polymorphism and Superconductivity in Bilayer Molecular Metals (CNB-EDT-TTF)$_4$I$_3$

Sandra Rabaça,*[,†] Sandrina Oliveira,[†] Isabel C. Santos,[†,‡] Vasco Gama,[†] Dulce Belo,[†] Elsa B. Lopes,[†] Enric Canadell,[§] and Manuel Almeida*[,†]

[†]C^{2}TN, Instituto Superior Técnico, Universidade de Lisboa Estrada Nacional 10, P-2695-066 Bobadela LRS, Portugal

[‡]CQE, Instituto Superior Técnico, Universidade de Lisboa Av. Rovisco Pais, P-1049-001 Lisboa, Portugal

[§]Institut de Ciencia de Materials de Barcelona (ICMAB-CSIC), Campus UAB, E-08193 Bellaterra, Spain

Supporting Information

ABSTRACT: Electrocrystallization from solutions of the dissymmetrical ET derivative cyanobenzene-ethylenedithio-tetrathiafulvalene (CNB-EDT-TTF) in the presence of triiodide I_3^- affords two different polymorphs (β'' and κ) with the composition (CNB-EDT-TTF)$_4$I$_3$, both with a bilayer structure of the donors. These polymorphs differ in the packing patterns (β''- and κ-type) of the donor molecules in each layer, in both cases with bifurcated C−N···H interactions effectively coupling head-to-head donor molecules between layer pairs. Two β'' polymorphs can be obtained with different degrees of anionic ordering. In one disordered phase, β''_d, with a smaller unit cell, the triiodide anions are disordered over two possible positions in a channel between the donor bilayers, while in the ordered phase, β''_o, the triiodide anions occupy only one of those positions in this channel, leading to the doubling of the unit cell in the layer plane. These results for β'' phases contrast with the κ polymorph previously reported, for which weaker disorder of the triiodide anions, over two possible orientations with 94 and 6% occupation factors, was observed. While the β'' polymorphs remains metallic down to 1.5 K with a ρ_{300K}/ρ_{4K} resistivity ratio of 250, the κ polymorph presents a much smaller resistivity ratio in the range of 4−10 and superconductivity with an onset temperature of 3.5 K.

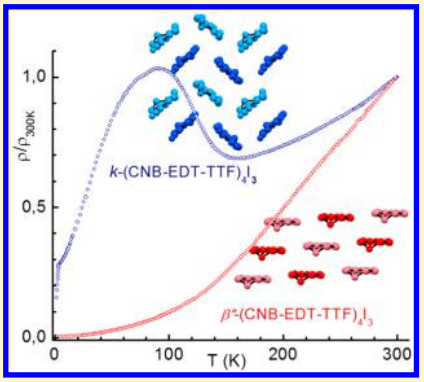

1. INTRODUCTION

The field of two-dimensional molecular systems has been largely dominated by charge transfer salts of sulfur rich derivatives of the electron donor tetrathiafulvalene (TTF). In these salts, the partially oxidized donor molecules are arranged in compact layers with their long axes parallel to each other, which alternate with anionic layers. BEDT-TTF (or ET = bis-ethylenedithio tetrathiafulvalene) is probably the most prolific of such donor molecules, but many other similar TTF derivatives have been used to prepare two-dimensional (2D) molecular systems. In all these donors, the presence of several sulfur atoms in the molecular periphery ensures significant electronic exchange interactions between neighboring molecules in the compact donor layers, while the interactions between layers are much weaker because of their separation by anions. These types of salts have been at the center of many studies because of a wealth of different possible ground states and phase transitions that have been observed, including antiferromagnetism, Mott insulator, charge ordering, 2D metallic, and even superconducting properties.[1−5] The physical properties of these 2D systems are critically dependent on the way the flat donor molecules are packed in a layer, which can be quite diverse and have been classified with many different Greek letters.[6−8]

Weak interactions such as halogen and hydrogen bonds have been extensively explored to control the donor packing pattern of charge transfer salts[9] with strong but not always easily predicted consequences for the electrical and magnetic properties of the salts. Recently, we have demonstrated that the dissymmetrical TTF derivative, cyanobenzene-ethylenedithio-tetrathiafulvalene (CNB-EDT-TTF),[10] when electrocrystallized in the presence of small anions A, such as I_3^-, ClO_4^-, or PF_6^-, leads to a series of salts with an unusual donor:anion stoichiometry of 4:1, with the general formula (CNB-EDT-TTF)$_4$A.[11] These salts are characterized by a bilayer structure of the donors, arranged in a head-to-head fashion between paired layers due to a specific combination of C−N···H−C interactions involving the cyano groups. In the bilayer salts of this donor with different anions, β''- and κ-type packing patterns of the CNB-EDT-TTF donors have previously been observed.

In this paper, we report for (CNB-EDT-TTF)$_4$I$_3$ two β''-type polymorphs, with a donor packing pattern similar to that observed in β''-ClO_4 and PF_6 salts but different degrees of anion order, in addition to the previously reported κ-type

Received: July 5, 2016
Published: September 28, 2016

DOI: 10.1021/acs.inorgchem.6b01555
Inorg. Chem. 2016, 55, 10343−10350

structure. κ-(CNB-EDT-TTF)$_4$I$_3$ displays superconductivity below 3 K, while the β'' polymorphs are regular 2D metals.[11]

2. EXPERIMENTAL SECTION

2.1. Sample Preparation. The electron donor CNB-EDT-TTF was prepared as previously described.[10] Crystals of β''-(CNB-EDT-TTF)$_4$I$_3$ were obtained by electrocrystallization, at room temperature, with platinum electrodes. A dichloromethane solution of the donor CNB-EDT-TTF (2×10^{-3} M) and TBAI$_3$ (6×10^{-3} M) was added to an H-shaped cell. The system was sealed under nitrogen, and the current was gradually increased from 0.2 to 0.5 μA cm^{-2} during the first 3 days of the electrocrystallization. After applying a constant current density of 0.5 μA cm^{-2} for approximately 18 days, we collected black elongated platelet-shaped crystals grown on the anode, with approximate dimensions of 5 mm × 0.2 mm × 0.05 mm, and washed the crystals with dichloromethane.

2.2. X-ray Crystallography. Selected single crystals were mounted on a loop with protective oil, and X-ray data were collected on a Bruker APEX II CCD detector diffractometer using graphite-monochromated Mo Kα radiation (λ = 0.71073 Å) and operating in φ and ω scan mode. A semiempirical absorption correction was performed using SADABS.[12] Data collection, cell refinement, and data reduction were conducted with SMART and SAINT.[13] The structures were determined by direct methods using SIR97[14] and refined by full-matrix least-squares methods using SHELXL97[15] using the winGX software package.[16] Non-hydrogen atoms were refined with anisotropic thermal parameters, whereas H atoms were placed in idealized positions and allowed to refine riding on the parent C atom. Molecular graphics were prepared using ORTEP 3.[17]

CCDC entry 1488030 and CCDC entry 1488031 contain the supplementary crystallographic data for this paper. These data can be obtained free of charge from The Cambridge Crystallographic Data Centre via www.ccdc.cam.ac.uk/data_request/cif.

2.3. Electrical Transport Measurements. Electrical resistivity was measured in the range of 1.5−300 K in a helium cryostat with an 18 T superconducting magnet (Oxford Instruments). Selected single crystals as elongated platelets were attached to 25 μm diameter Au wires with Pt paint (Demetron 308A), in a 4 in. line configuration of the contacts placed along the long axis of the samples that correspond to the donor stacking axis. The ac (77 Hz) current was kept in the range of 1−10 μA, and the sample voltage drop was measured by a lock-in amplifier (Stanford Research Systems model SR830).

Thermoelectric power measurements in single crystals were performed also along the long axis of the samples in the temperature range of 20−300 K in a closed-cycle helium refrigerator using a slow alternating current (~10^{-2} Hz) technique[18] by attaching two 25 μm diameter 99.99% pure Au wires (Goodfellow metals) thermally anchored to two quartz reservoirs with Pt paint (Demetron 308A) to the extremities of an elongated sample, as in a previously described apparatus,[19] controlled by a computer.[20] The oscillating thermal gradient was kept below 1 K and was measured with a differential Au (0.05 atom % Fe) versus the chromel thermocouple. The absolute thermoelectric power of the sample was obtained after correction for the absolute thermopower of the Au leads by using the data of Huebner.[21]

2.4. Computational Details. The tight-binding band structure calculations[22] were of the extended Hückel type, and a modified Wolfsberg−Helmholtz formula was used to calculate the nondiagonal $H_{\mu\nu}$ values.[23] All valence electrons were taken into account in the calculations, and the basis set consisted of Slater-type orbitals of double-ζ quality for C and N 2s and 2p, and S 3s and 3p and of single-ζ quality for H 1s. The ionization potentials, contraction coefficients, and exponents were taken from previous work.[24,25]

3. RESULTS AND DISCUSSION

3.1. Crystal Structure. X-ray diffraction of selected (CNB-EDT-TTF)$_4$I$_3$ single crystals obtained by electrocrystallization revealed two new crystal structures, both with the same bilayer β''-type arrangement of the donors, but with different degrees of disorder in the positions of the triiodide anions (Table 1).

Table 1. Crystal and Refinement Data for β''_d-(CBN-EDT-TTF)$_4$I$_3$ and β''_o-(CBN-EDT-TTF)$_4$I$_3$

	β''_d-(CBN-EDT-TTF)$_4$I$_3$	β''_o-(CBN-EDT-TTF)$_4$I$_3$
chemical formula	$C_{26}H_{14}I_{1.5}N_2S_{12}$	$C_{52}H_{28}I_3N_4S_{24}$
molecular mass	929.46	1858.92
T (K)	150(2)	150(2)
dimensions (mm)	0.40 × 0.04 × 0.02	0.60 × 0.03 × 0.01
crystal color	black	black
crystal system	triclinic	triclinic
space group	$P\bar{1}$	$P\bar{1}$
a (Å)	4.8597(9)	5.7669(2)
b (Å)	5.7697(11)	9.7113(3)
c (Å)	27.733(5)	27.7724(7)
α (deg)	89.033(6)	86.793(2)
β (deg)	87.007(6)	89.0790(10)
γ (deg)	84.443(7)	84.558(2)
volume (Å^3)	772.8(2)	1545.84(8)
Z	1	1
ρ_{calc} (g cm^{-3})	2.133	1.997
μ (mm^{-1})	2.371	2.371
h, k, l range	±5, −6/7, ±33	±6, −11/+10, ±33
θ_{max} (deg)	25.87	25.35
no. of reflections collected	3831	19649
no. of unique reflections	2542 (R_{int} = 0.0354)	5303 (R_{int} = 0.0527)
data/restraints/parameters	2542/0/195	5303/12/377
goodness of fit on F^2	1.054	1.065
R_1; ωR_2 [$I > 2\sigma(I)$]	0.0640; 0.1303	0.0892; 0.2263
largest difference peak and hole (e Å^{-3})	1.286 and −1.165	4.998 and −2.676
CCDC entry	1488031	1488030

[a]Crystallographic data (excluding structure factors) for β''_d-(CBN-EDT-TTF)$_4$I$_3$ and β''_o-(CBN-EDT-TTF)$_4$I$_3$ were deposited with the Cambridge Crystallographic Data Centre as entries 1488031 and 1488030, respectively.

No crystals with the previously reported κ-type structure were obtained, and it was not clear which specific electrocrystallization conditions favor the crystallization of the different phases. In one structure called β''_d-(CNB-EDT-TTF)$_4$I$_3$, the unit cell is triclinic, $P\bar{1}$, with the following cell parameters: a = 4.8597(9) Å, b = 5.7697(11) Å, c = 27.733(5) Å, α = 89.033(6)°, β = 87.007(6)°, γ = 84.443(7)°, and V = 772.841 Å^3. The asymmetric unit is composed of one donor molecule and two iodine atoms at special positions with occupation factors of 0.694 and 0.831 for I1 and I2, respectively.

Another structure called β''_o-(CNB-EDT-TTF)$_4$I$_3$ is also triclinic, $P\bar{1}$, but with the following cell parameters: a = 5.7669(2) Å, b = 9.7113(3) Å, c = 27.7724(7) Å, α = 86.793(2)°, β = 89.079(1)°, γ = 84.558(2)°, and V = 1545.84(5) Å^3. This unit cell has twice the volume of the previous one, with cell parameter b corresponding to a doubling of the previous cell parameter a. The asymmetric unit is composed of two donor molecules and two iodine atoms in fully occupied positions. One of the iodine atoms is located on an inversion center and the other at a general position.

The donor packing of both β''_d and β''_o structures is essentially the same as shown in Figure 1, and it is also identical to that previously described in ClO_4 and PF_6 salts with a bilayer β''-type packing of the donors.[4] The CNB-EDT-TTF

DOI: 10.1021/acs.inorgchem.6b01555
Inorg. Chem. 2016, 55, 10343−10350

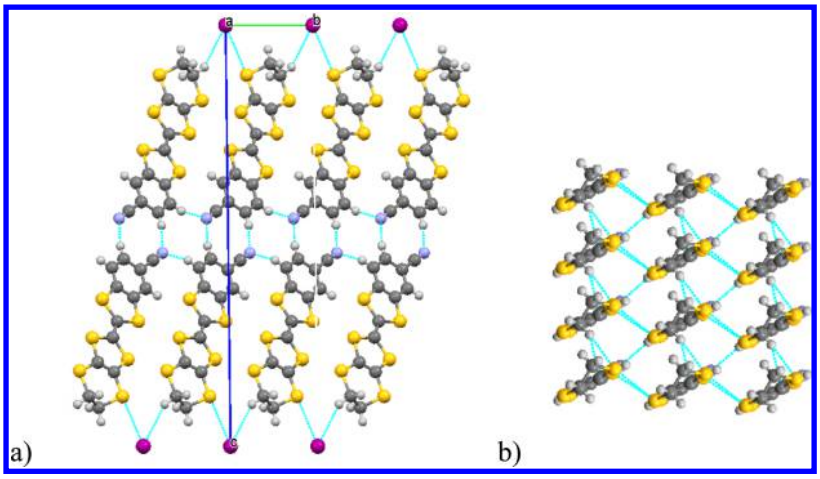

Figure 1. (a) β''_d-(CNB-EDT-TTF)$_4$I$_3$ structure viewed along the *a* axis. (b) Partial view of one donor layer along the molecule long axis showing a β''-type molecular packing pattern.

molecules do not present any disorder in the dithiine ring as previously observed in the PF_6 salt[11] and commonly found in many ET salts.[1,5] These donors are arranged in a head-to-head fashion in bilayers through dipolar and bifurcated C−N···H interactions, which can be described as a combination of dimeric $R^2_2(10)$ and $R^2_4(10)$ synthons, in Etter's notation,[26−28] connecting almost coplanar molecules (Figures 1a).

Similar synthons are quite common in molecules with nitrile groups,[29] and it is worth mentioning that a dimeric $R^2_2(10)$ synthon has been previously observed in a 1:1 salt of the cyano-substituted TTF 3-cyano-3′,4′-ethylenedithiotetrathiafulvalene (EDT-TTF-CN), (EDT-TTF-CN)I_3, however, without the $R^2_4(10)$ synthons that in the CNB-EDT-TTF salts ensure the bilayer structure.

In β''_d-(CNB-EDT-TTF)$_4$I$_3$, the iodine atoms appear in two positions I1 and I2, located in channels between the donor bilayers (Figure 2) with anomalously large displacement

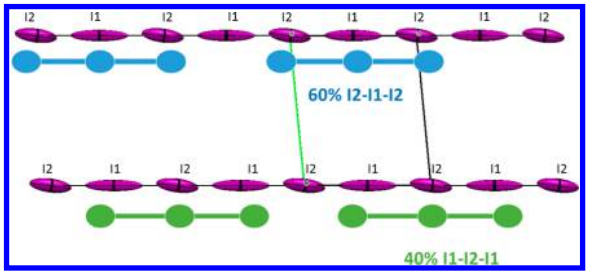

Figure 2. ORTEP diagram of iodine atom positions (violet) in the *a*−*c* anionic layer of β''_d-(CNB-EDT-TTF)$_4$I$_3$ drawn at the 50% probability level. In blue and green are schematically depicted two possible locations for the triiodide anions along the chains of iodine atom positions, which with occupations factors of ∼60 and 40% account for the observed occupation factors of 0.694 and 0.831 for I1 and I2, respectively.

parameters along the channels (cell axis *b*) and occupation factors of 0.694 and 0.831, respectively. These occupation factors, corresponding to 1.525 iodine atoms for 2 donors, are very close to the expected value for a 4:1 (donor:I_3^-) stoichiometry in these compounds. The distance between these iodine positions, 2.429 Å, is slightly shorter than the typical I−I distance in triiodide (2.92 Å), which cannot be precisely accommodated in these positions, and the elongated displacement parameter ellipsoids denote position disorder of triiodide anions. Therefore, this structure with a small unit cell parameter *a* should be regarded as an average structure involving disorder of triiodide anions. The repeat length of the anions in this chain of iodine positions cannot be smaller than the triiodide length (∼9 Å), and in other channel structures, it is observed to occur typically with repeats in the range of 9.4−9.9 Å,[30−32] close to the doubling of unit cell parameter *a*. In fact, the occupation factors of these two iodine positions in the β''_d-(CNB-EDT-TTF)$_4$I$_3$ structure can be seen as resulting from a superposition of a random occupation of these sites by triiodide anions, 60% in positions close to the I2−I1−I2 portion and 40% in positions close to the I1−I2−I1 portion as schematically depicted in blue and green in Figure 2. It should also be noted that iodine atoms at positions I1 and I2 present slightly different environments in the channel between donors; I1 has two short contacts with S6 sulfur atoms of 3.649 Å, while the shortest contacts of I2 are with H13 at 3.094 Å.

The asymmetric unit of β''_o-(CNB-EDT-TTF)$_4$I$_3$ contains two donor molecules and half a triiodide anion with the central iodine atom at an inversion center. The β''_o-(CNB-EDT-TTF)$_4$I$_3$ structure presents the same packing pattern of donors as the disordered β''_d phase, however with a doubling of the cell parameter along the channel of the iodine positions and with the iodine atoms in ordered positions, very close to the preferred I2−I1−I2 positions of the disordered β''_d phase. As a consequence of this anion ordering and cell doubling, the donor units become inequivalent with one molecule A (blue) in closer contact with anions than the other unit B (red) (Figure 3). Donor molecule A bearing shorter anionic contacts (S5−I1 at 3.669 Å and H13A−I2 at 3.071 Å) is expected to present a larger positive charge. The analysis of donor bond lengths in molecules A and B shows small differences consistent with such a possibility. However, these differences are within the experimental uncertainties, precluding at this point a more positive conclusion about donor charge distribution.

3.2. Electronic Structure. The structure with disordered anions β''_d-(CNB-EDT-TTF)$_4$I$_3$ contains one bilayer with only one donor molecule as the repeat unit for every single layer. As shown in Figure 4, in this average structure, there are three different types of intermolecular interactions among molecules in the same layer: those along the π stacks in the *a* direction (I), the lateral contacts along the *a* + *b* direction (II), and those along the step chains in the *b* direction (III). As shown in Table 2, the stronger HOMO···HOMO intermolecular interactions[33]

DOI: 10.1021/acs.inorgchem.6b01555
Inorg. Chem. 2016, 55, 10343−10350

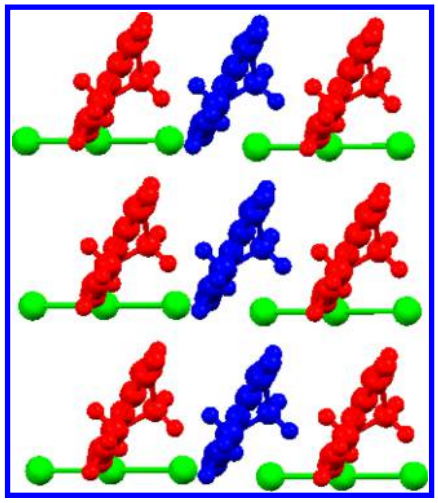

Figure 3. Partial view along the molecule long axis of one donor layer in β''_o-(CNB-EDT-TTF)$_4$I$_3$ showing two inequivalent donor units colored blue (molecule A) and red (molecule B).

are those along the step chains whereas those along the π stacks are approximately half as strong. Note that the lateral interactions despite being associated with the shorter S···S contacts are the weakest because they are associated with usually weak π-type interactions whereas those along the step chains or the π stacks are of the stronger σ type. The interaction between donors in different layers of the bilayer (IV) is very weak (0.6 meV). These values are very similar to those previously reported for the isostructural (CNB-EDT-TTF)$_4$X salts, where X = PF_6 and ClO_4.[5] Note that the relative strength of the interactions along the π stacks and the lateral interactions is reversed with respect to those of most β'' salts.[34]

The calculated band structure and Fermi surface assuming a $+^1/_4$ charge for the donor molecules are shown in Figure 5. As usual for β'' salts,[34] the Fermi surface has a closed ellipse-like shape centered at the border of the Brillouin zone along the a^* direction (a being the direction of the π stacks) for every layer. The orientation and shape of this ellipse depend on the relative strength of the three different interactions.[34] Because the interaction of the layers is very weak, the area of each ellipse is practically $^1/_8$ of the cross section of the Brillouin zone. Thus, if the average structure provides a good description of the system, it is predicted that magnetoresistance measurements should exhibit Shubnikov−de Haas oscillations with frequencies of $^1/_8$ of the cross section of the Brillouin zone.

Table 2. Calculated Values of $|\beta_{HOMO-HOMO}|$ (electronvolts) for the Different Donor···Donor Interactions in β''_d-(CNB-EDT-TTF)$_4$I$_3$ and β''_o-(CNB-EDT-TTF)$_4$I$_3$

	$\lvert\beta_{HOMO-HOMO}\rvert$ (meV)	
interaction type	β''_d-(CNB-EDT-TTF)$_4$I$_3$	β''_o-(CNB-EDT-TTF)$_4$I$_3$
I	125.0	90.9
		162.3
II	51.2	50.6
		50.4
III	219.6	218.0
		207.7
IV	0.6	0.6

The structure with ordered anions, β''_o-(CNB-EDT-TTF)$_4$I$_3$, contains one bilayer with two donor molecules as the repeat unit for every single layer. As shown in Figure 4, in this structure, there are six different types of intermolecular interactions, two of each type previously described. Note that the direction of the π stacks is now b whereas the direction of the step layers is a. As shown in Table 2, it is only for the interactions along the π stacks (I and I′) that cell doubling has an important effect; those along the other directions are practically not affected.

The doubling along the π stacks and the induced sizable differentiation of the interactions along such a direction lead to a large splitting of the two pairs of bands along all directions of the Brillouin zone (see Figure 6, left), so that one pair of bands is completely filled and the other pair is one-quarter empty, ultimately leading to the warped but open Fermi surface shown in the right panel of Figure 6. This is in stark contrast to the closed Fermi surface calculated for the average structure of the anion-disordered structure. However, the shape of this Fermi surface can be easily rationalized by noting that the main difference between the ordered and disordered anion structures is a doubling along the direction of the π stacks. Consequently, as shown in Figure 7, the Fermi surface of the ordered anion phase can be approximated by folding the Fermi surface of the disordered anion structure along a^* (which will become b^* in the ordered phase because of the labeling change). Because of the folding and the variation in the interaction strength along the π stack direction, the successive ellipses only slightly touch, and this is why a pair of warped open lines is generated. If the area of the ellipses had been larger, their overlap would had been larger, and in addition to the warped open lines, a new and smaller closed pocket would have been generated in that region.[34]

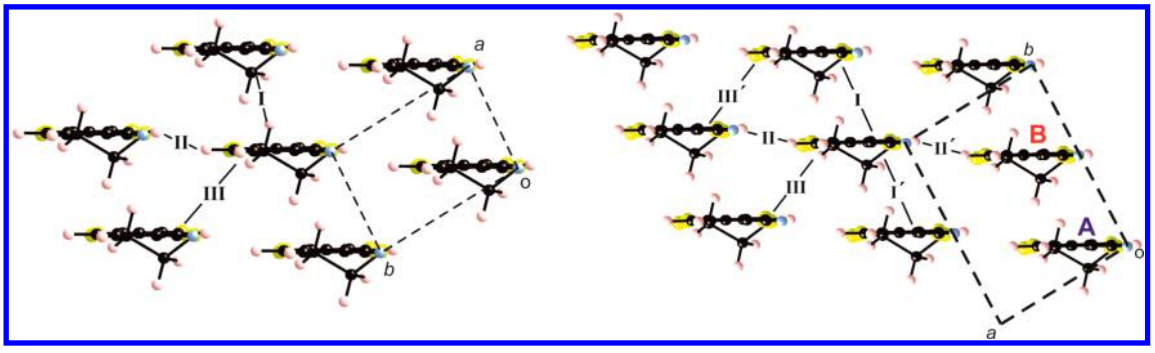

Figure 4. Donor layer in bilayers of β''_d-(CNB-EDT-TTF)$_4$I$_3$ (left) and β''_o-(CNB-EDT-TTF)$_4$I$_3$ (right), where the different interactions are labeled.

DOI: 10.1021/acs.inorgchem.6b01555
Inorg. Chem. 2016, 55, 10343−10350

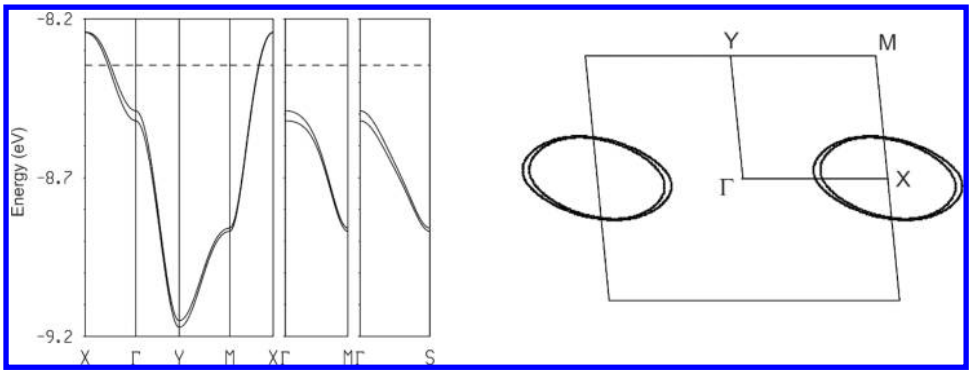

Figure 5. Calculated electronic band structure (left) and Fermi surface (right) for the donor bilayer of the anion-disordered structure β''_d-(CNB-EDT-TTF)$_4$I$_3$, assuming a $+^1/_4$ charge per donor. The dashed line in the band structure refers to the Fermi level; Γ = (0, 0), X = (a*/2, 0), Y = (0, b*/2), and M = (a*/2, b*/2).

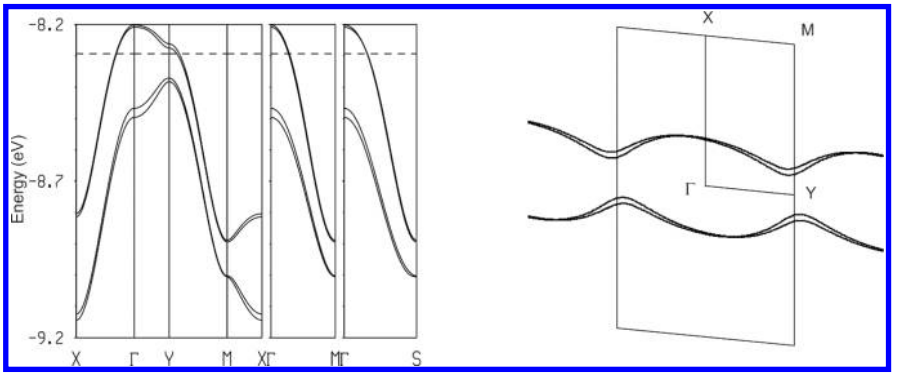

Figure 6. Calculated electronic band structure (left) and Fermi surface (right) for the donor bilayer of β''_o-(CNB-EDT-TTF)$_4$I$_3$. The dashed line in the band structure refers to the Fermi level; Γ = (0, 0), X = (a*/2, 0), Y = (0, b*/2), and M = (a*/2, b*/2).

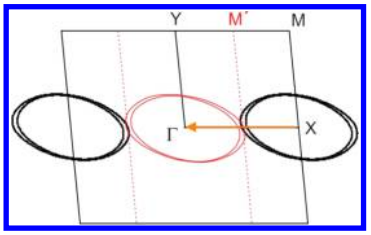

Figure 7. Schematic construction of the open Fermi surface of the anion-ordered structure β''_o-(CNB-EDT-TTF)$_4$I$_3$ from that of the anion-disordered structure by a folding process. Note the different axis labeling in the two structures.

The absence of closed portions of the Fermi surface in the anion-ordered structure of β''_o-(CNB-EDT-TTF)$_4$I$_3$ leads to the prediction that no Shubnikov–de Haas oscillations should be observed in the low-temperature magnetoresistance measurements. This is in agreement with the experimental magnetoresistance studies. The fact that such oscillations have not been observed for the (CNB-EDT-TTF)$_4$X salts for which X = PF_6 and ClO_4 also exhibiting a β''-type structure strongly suggests that the presently known structures for these anions are only average structures as in the present case.

3.3. Electron Transport Properties. The β''_d and β''_o structures described above are specific cases of disordered and ordered anions, but other intermediately disordered situations probably exist in the crystals. Real crystals may even present domains with different degrees of anion ordering. The electrical conductivity and thermoelectric power of several crystals coming from different preparations were measured, and in nine samples, no significant differences that could be ascribed to different degrees of anions ordering could be observed in the temperature dependence of both electrical conductivity and thermoelectric power. The behavior of the β''-type crystals is, however, strikingly different from that of the κ-phase crystals obtained in previous preparations.

Electrical conductivity of β'' crystals measured along the long dimension of the elongated plate-shaped crystals (donor stacking axis) was found in the range of 30–110 S/cm at room temperature. This range of values is believed to reflect mainly the difficulty in accurately measuring the thickness of the small platelet-shaped crystals, rather than possible variable degrees of anion ordering. In all samples, the electrical resistivity, ρ, decreases upon cooling in the same regular metallic fashion with a resistivity ratio between 300 and 4 K (ρ_{300K}/ρ_{4K}) reaching values of approximately 120–250 depending on the sample quality.

The electrical conductivity of κ crystals at room temperature (24 S/cm) is slightly below that of the β'' phases, and most significantly, it presents a different temperature dependence (Figure 8).[11] When samples are cooled from room temperature, there is first a metallic decrease in resistivity, ρ, although not so fast as in the β'' phases. This initial decrease in resistivity is, however, followed by an anomalous increase upon cooling starting around 150 K and reaching a maximum at ~100 K, followed by a final decrease upon further cooling. The magnitude of the maximum in this resistivity hump was found to be sample-dependent, reaching in some samples values well above the room-temperature value. This anomalous hump has been previously thought to be possibly associated with charge ordering,[5] but its origin remains unclear. It is worth

DOI: 10.1021/acs.inorgchem.6b01555
Inorg. Chem. 2016, 55, 10343–10350

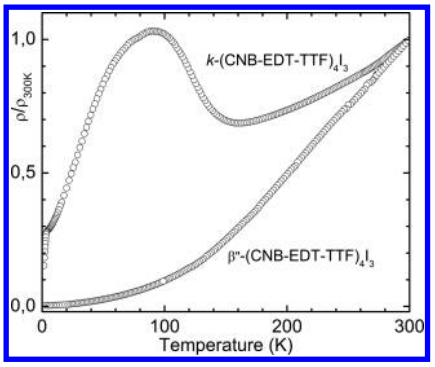

Figure 8. Temperature dependence of the electrical resistivity of $(CNB\text{-}EDT\text{-}TTF)_4I_3$ single crystals.

mentioning that a similar behavior has been observed in other ET iodine salts such as γ-$(ET)_3(I_3)_{2.5}$.[35]

κ crystals below liquid helium temperatures exhibit a sharp decrease in their electrical resistivity upon cooling starting at ~3.5 K, which is completely suppressed by the application of magnetic fields as small as 0.5 T (Figure 9). This decrease in

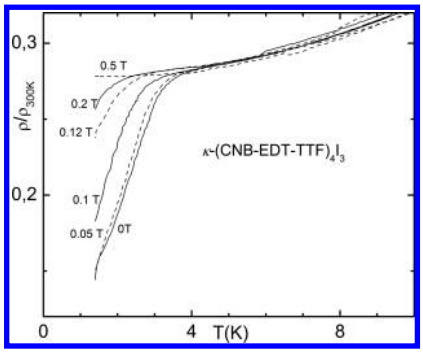

Figure 9. Low-temperature dependence of the electrical resistivity of κ-$(CNB\text{-}EDT\text{-}TTF)_4I_3$ single crystals under different magnetic fields.

electrical resistivity does not reach zero (resistivity at 1.5 K under zero field is still ~35% of the value at 4 K), indicating an incomplete superconducting transition with an onset temperature of ~3.5 K and a critical field of 360 mT at 1.5 K (Figure S1). This behavior of the κ crystals contrasts with that of the β'' crystals, which show no indication of superconductivity down to 1.5 K. In both κ- and β''-phase crystals, no signs of any oscillation were found in the magnetoresistance at 1.5 K under fields of up to 18 T. The magnetoresistance at 1.4 K just shows a regular behavior with positive values of ~2.5% per tesla up to 16 T in the case of the β'' crystals and ~0.8% per tesla up to 16 T in the case of the κ crystals.

The thermoelectric power, S, of β'' crystals, 75 $\mu V\ K^{-1}$ at room temperature, shows a behavior comparable to that previously reported for β''-$(CNB\text{-}EDT\text{-}TTF)_4ClO_4$ and β''-$(CNB\text{-}EDT\text{-}TTF)_4PF_6$, with large positive values consistent with the large band filling (7/8) of these 4:1 salts and quite different from that of κ-$(CNB\text{-}EDT\text{-}TTF)_4I_3$ (with half-filled bands), 30 $\mu V\ K^{-1}$ at room temperature.[11] The absolute thermoelectric power of β''-$(CNB\text{-}EDT\text{-}TTF)_4I_3$ crystals decreases regularly upon cooling (Figure 10), first almost proportionally with temperature as in a regular metal, but below 200 K, it starts to decrease faster, crossing zero at 93 K to reach -5 $\mu V\ K^{-1}$ at 60 K and then staying almost temperature-independent down to 22 K. The larger thermoelectric power of

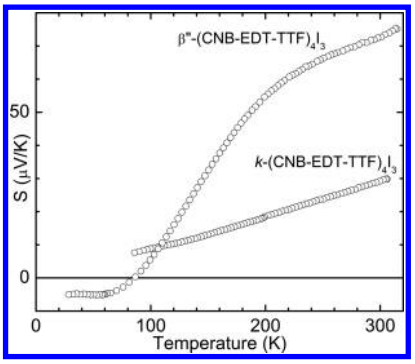

Figure 10. Temperature dependence of the absolute thermoelectric power of $(CNB\text{-}EDT\text{-}TTF)_4I_3$ single crystals.

the β'' crystals at room temperature when compared with that of the κ crystals reflects the larger band filling of the first phases. A quite similar temperature dependence of thermoelectric power with sign change upon cooling has been reported in β-$(BEDT\text{-}TTF)_2I_3$, although with smaller values because of the smaller band filling of the 2:1 salt.[36,37] This change in sign of thermoelectric power in β-$(BEDT\text{-}TTF)_2I_3$ at low temperatures was interpreted within a simple band model as being a consequence of the 2D Fermi surface with points very close to the zone boundary[38] in a situation close to the predictions for β''-$(CNB\text{-}EDT\text{-}TTF)_4I_3$.

4. CONCLUSIONS

In conclusion, our results show that the well-known polymorphism associated with donor packing pattern variation in single-layer ET salts is also present in bilayer salts of CNB-EDT-TTF. For $(CNB\text{-}EDT\text{-}TTF)_4I_3$, at least two type of polymorphs characterized by β''- and κ-type packing patterns of donors have been observed with the same triiodide anions. κ-$(CNB\text{-}EDT\text{-}TTF)_4I_3$ displays superconductivity below 3 K, while β''-$(CNB\text{-}EDT\text{-}TTF)_4I_3$ crystals remain regular metals down to 1.5 K with a large resistivity ratio (ρ_{300K}/ρ_{4K}). In addition to the donor packing pattern variations, in β''-$(CNB\text{-}EDT\text{-}TTF)_4I_3$, different degrees of anion ordering over two possible positions of the I_3^- anions are possible. A unit cell doubling associated with triiodide anion ordering in these positions is observed. In principle, the variable anion order/disorder could affect the shape of the Fermi surface. However, no significant variable disorder effects were detected in the electrical transport properties of different single crystals. The experimental conditions favoring the preparation of any of these polymorphs remain undetermined. Our results most probably just anticipate the possibility of a much larger structural diversity and richer polymorphism in bilayer salts of CNB-EDT-TTF.

■ ASSOCIATED CONTENT

Supporting Information

The Supporting Information is available free of charge on the ACS Publications website at DOI: 10.1021/acs.inorgchem.6b01555.

Crystallographic data (CIF)
Crystallographic data (CIF)
Additional observations and data (PDF)

DOI: 10.1021/acs.inorgchem.6b01555
Inorg. Chem. 2016, 55, 10343−10350

AUTHOR INFORMATION

Corresponding Authors

*Phone: +351 219946171. E-mail: malmeida@ctn.tecnico.ulisboa.pt.

*Phone: +351 219946203. E-mail: sandrar@ctn.tecnico.ulisboa.pt.

Notes

The authors declare no competing financial interest.

ACKNOWLEDGMENTS

This work was partially supported in Portugal by FCT under Contracts UID/Multi/04349/2013 and RECI/QEQ-QIN/0189/2012 and grants to S.O. (SFRH/BD/72722/2010) and S.R. (SFRH/BPD/113344/2015). Work in Bellaterra was supported by MINECO-Spain (Grant FIS2015-64886-C5-4-P) and Generalitat de Catalunya (2014SGR301). E.C. acknowledges the support of the Spanish MINECO through the Severo Ochoa Centers of Excellence Program under Grant SEV-2015-0496.

REFERENCES

(1) Ishiguro, T.; Yamaji, K.; Saito, G. *Organic Superconductors*, 2nd ed.; Springer-Verlag: Berlin, 1998.

(2) Seo, H.; Hotta, C.; Fukuyama, H. Toward Systematic Understanding of Diversity of Electronic Properties in Low-Dimensional Molecular Solids. *Chem. Rev.* **2004**, *104*, 5005−5036.

(3) Jerome, D. Organic Conductors: From Charge Density Wave TTF−TCNQ to Superconducting $(TMTSF)_2PF_6$. *Chem. Rev.* **2004**, *104*, 5565−5592.

(4) Seo, H. Charge Ordering in Organic ET Compounds. *J. Phys. Soc. Jpn.* **2000**, *69*, 805−820.

(5) Williams, J. M.; Ferraro, J.; Torn, R. J.; Carlson, K. D.; Geiser, U.; Wang, H. H.; Kini, A. M.; Whangbo, M.-H. *Organic Superconductors (including Fullerenes)*; Prentice Hall: Englewood Cliffs, NJ, 1992.

(6) Mori, T. Structural Genealogy of BEDT-TTF-Based Organic Conductors I. Parallel Molecules: β and β'' Phases. *Bull. Chem. Soc. Jpn.* **1998**, *71*, 2509−2526.

(7) Mori, T.; Mori, H.; Tanaka, S. Structural Genealogy of BEDT-TTF-Based Organic Conductors II. Inclined Molecules: θ, α, and κ Phases. *Bull. Chem. Soc. Jpn.* **1999**, *72*, 179−197.

(8) Mori, T. Structural Genealogy of BEDT-TTF-Based Organic Conductors III. Twisted Molecules: δ and α' Phases. *Bull. Chem. Soc. Jpn.* **1999**, *72*, 2011−2027.

(9) Fourmigue, M.; Batail, P. Activation of Hydrogen- and Halogen-Bonding Interactions in Tetrathiafulvalene-Based Crystalline Molecular Conductors. *Chem. Rev.* **2004**, *104*, 5379−5418.

(10) Oliveira, S.; Belo, D.; Santos, I. C.; Rabaça, S.; Almeida, M. Synthesis and Characterization of the Cyanobenzene-Ethylenedithio-TTF Donor. *Beilstein J. Org. Chem.* **2015**, *11*, 951−956.

(11) Oliveira, S.; Ministro, J.; Santos, I. C.; Belo, D.; Lopes, E. B.; Rabaça, S.; Canadell, E.; Almeida, M. Bilayer Molecular Metals Based on Dissymmetrical Electron Donors. *Inorg. Chem.* **2015**, *54*, 6677−6679.

(12) Sheldrick, G. M. *SADABS*; Bruker AXS Inc.: Madison, WI, 2004.

(13) *SMART and SAINT*; Bruker AXS Inc.: Madison, WI, 2004.

(14) Altomare, A.; Burla, M. C.; Camalli, M.; Cascarano, G.; Giacovazzo, G.; Guagliardi, A.; Moliterni, A. G. G.; Polidori, G.; Spagna, R. SIR97: a New Tool for Crystal Structure Determination and Refinement. *J. Appl. Crystallogr.* **1999**, *32*, 115−119.

(15) Sheldrick, G. M. *SHELXL97, Program for Crystal Structure Refinement*; University of Göttingen: Göttingen, Germany, 1997.

(16) Farrugia, L. J. WinGX Suite for Small-Molecule Single-Crystal Crystallography. *J. Appl. Crystallogr.* **1999**, *32*, 837−838.

(17) Farrugia, L. J. ORTEP-3 for Windows a Version of ORTEP-III with a Graphical User Interface (GUI). *J. Appl. Crystallogr.* **1997**, *30*, 565.

(18) Chaikin, P. M.; Kwak, J. F. Apparatus for Thermopower Measurements on Organic Conductors. *Rev. Sci. Instrum.* **1975**, *46*, 218.

(19) Almeida, M.; Alcácer, L.; Oostra, S. Anisotropy of Thermopower in N-methyl-N-Ethylmorpholinium Bistetracyanoquinodimethane, $MEM(TCNQ)_2$, in the Region of the High-Temperature Phase Transitions. *Phys. Rev. B: Condens. Matter Mater. Phys.* **1984**, *30*, 2839−2844.

(20) Lopes, E. B. INETI-Sacavém, internal report, 1991.

(21) Huebener, R. P. Thermoelectric Power of Lattice Vacancies in Gold. *Phys. Rev.* **1964**, *135*, A1281−A1291.

(22) Whangbo, M.-H.; Hoffmann, R. The Band Structure of the Tetracyanoplatinate Chain. *J. Am. Chem. Soc.* **1978**, *100*, 6093−6098.

(23) Ammeter, J. H.; Bürgi, H.-B.; Thibeault, J.; Hoffmann, R. Counterintuitive Orbital Mixing in Semiempirical and ab Initio Molecular Orbital Calculations. *J. Am. Chem. Soc.* **1978**, *100*, 3686−3692.

(24) Pénicaud, A.; Boubekeur, K.; Batail, P.; Canadell, E.; Auban-Senzier, P.; Jérome, D. Hydrogen-Bond Tuning of Macroscopic Transport Properties from the Neutral Molecular Component Site Along the Series of Metallic Organic-Inorganic Solvates $(BEDT\text{-}TTF)_4Re_6Se_5Cl_9$.[guest], [guest = DMF, THF, Dioxane]. *J. Am. Chem. Soc.* **1993**, *115*, 4101−4112.

(25) Baudron, S. A.; Avarvari, N.; Canadell, E.; Auban-Senzier, P.; Batail, P. Structural Isomerism in Crystals of Redox-Active Secondary Ortho-Diamides: The Role of Competing Intra and Intermolecular Hydrogen Bonds in Directing Crystalline Topologies. *Chem. - Eur. J.* **2004**, *10*, 4498−4511.

(26) Etter, M. C.; MacDonald, J. C.; Bernstein, J. Graph-Set Analysis of Hydrogen-Bond Patterns in Organic Crystals. *Acta Crystallogr., Sect. B: Struct. Sci.* **1990**, *46*, 256−262.

(27) Etter, M. C. Encoding and Decoding Hydrogen-Bond Patterns of Organic Compounds. *Acc. Chem. Res.* **1990**, *23*, 120−126.

(28) Etter, M. C. Hydrogen Bonds as Deslgn Elements in Organic Chemistry. *J. Phys. Chem.* **1991**, *95*, 4601−4610.

(29) Guth, H.; Heger, G.; Druck, U. Neutron diffraction study of the structure of p-benzenedicarbonitrile. *Z. Kristallogr. - Cryst. Mater.* **1982**, *159*, 185−190.

(30) Coppens, P. In *Extended Linear Chain Compounds*; Miller, J. S., Ed.; Plenum Press: New York, 1982; Vol. *1*, Chapter 7.

(31) Herbstein, F. H.; Kaftory, M.; Kapon, M.; Saenger, W. Structures of Three Crystals Containing Approximately Linear Chains of Triiodide Ions. *Z. Kristallogr. - Cryst. Mater.* **1981**, *154*, 11−30.

(32) Morgado, J.; Santos, I. C.; Henriques, R. T.; Fourmigué, M.; Matias, P.; Veiros, L. F.; Calhorda, M. J.; Duarte, M. T.; Alcacer, L.; Almeida, M. Molecular Metals Based on 1,2,7,8-Tetrahydrodicyclopenta[cd:lm]perylene and Iodine, $(CPP)_2(I_3)_{1-\delta}$. *Chem. Mater.* **1994**, *6*, 2309−2316.

(33) Whangbo, M.-H.; Williams, J. M.; Leung, P. C. W.; Beno, M. A.; Emge, T. J.; Wang, H. H. Role of the Intermolecular Interactions in the Two-Dimensional Ambient-Pressure Organic Superconductors β-$(ET)_2I_3$ and β-$(ET)_2IBr_2$. *Inorg. Chem.* **1985**, *24*, 3500−3502.

(34) Rousseau, R.; Gener, M.; Canadell, E. Step-by-Step Construction of the Electronic Structure of Molecular Conductors: Conceptual Aspects and Applications. *Adv. Funct. Mater.* **2004**, *14*, 201−214.

(35) Yagubskii, E. B.; Schegolev, I. F.; Topnoikov, V. N.; Pesotskii, S. I.; Laukhin, V. N.; Konovitch, P. A.; Kartsovnik, M. V.; Zvarykina, A. V. Superconducting Properties of the Orthorhombic Phase of bBis-(Ethylenedithiolo)Tetrathiofulvalene Triiodide. *JETP Letters* **1984**, *39*, 328−332.

(36) Mortensen, K.; Williams, J. M.; Wang, H. H. Anisotropic Thermopower of the Organic Metal, β-$(BEDT\text{-}TTF)_2I_3$. *Solid State Commun.* **1985**, *56*, 105−110.

(37) Merzhanov, V. A.; Kostyuchenko, E. E.; Faber, O. E.; Shchegolev, I. F.; Yagubskii, E. B. Thermoelectric and magnetic properties of the α- and β-modifications of $(BEDT\text{-}TTF)_2I_3$. *Sov. Phys., JETP* **1985**, *62*, 165.

DOI: 10.1021/acs.inorgchem.6b01555
Inorg. Chem. 2016, 55, 10343−10350

(38) Mori, T.; Inokuchi, H. Thermoelectric Power of Organic Superconductors − Calculation on the Basis of the Tight-Binding Theory. *J. Phys. Soc. Jpn.* **1988**, *57*, 3674−3677.

DOI: 10.1021/acs.inorgchem.6b01555
Inorg. Chem. 2016, 55, 10343−10350